Hindawi
Cellular Microbiology
Volume 2023, Article ID 2822094, 16 pages
https://doi.org/10.1155/2023/2822094

Research Article

Kluyveromyces marxianus Ameliorates High-Fat-Diet-Induced Kidney Injury by Affecting Gut Microbiota and TLR4/NF-κB Pathway in a Mouse Model

Na Li, Guanjie Zhao, and Mingzhu Xu

Department of Nephrology, China-Japan Union Hospital of Jilin University, Changchun 130033, China

Correspondence should be addressed to Mingzhu Xu; ms002@jlu.edu.cn

Received 21 August 2022; Revised 13 November 2022; Accepted 12 December 2022; Published 8 February 2023

Academic Editor: Jayaprakash Kolla

Objectives. The effects of *Kluyveromyces marxianus* on high-fat diet- (HFD-) induced kidney injury (KI) were explored. *Methods*. HFD-induced KI model was established using male C57BL/6 mice and treated with *K. marxianus* JLU-1016 and acid-resistant (AR) strain JLU-1016A. Glucose tolerance was evaluated via an oral glucose tolerance test (OGTT). KI was measured using Hematoxylin and Eosin (H&E) staining and terminal deoxynucleotidyl transferase dUTP nick end labeling (TUNEL) analysis. The chemical indexes were analyzed, including lipid profiles, inflammatory cytokines, and creatinine. The levels of Toll-like receptor 4 (TLR4)/nuclear factor kappa B (NF-κB) or phospho-NF-κB p65 (Ser536) and alpha inhibitor of NF-κB (IκBα) were measured using qPCR and Western blot. The gut microbiota was sequenced using high-throughput sequencing. *Results*. HFD induction increased OGTT value, KI severity, oxidative stress, inflammatory cytokines, oxidative stress, apoptotic rate, creatinine levels, and the expression of TLR4/NF-κB, phospho-NF-κB p65 (Ser536), and IκBα deteriorated lipid profiles ($P < 0.05$) and reduced gut microbiota abundance. *K. marxianus* treatment ameliorated HFD-induced metabolic disorders and reversed these parameters ($P < 0.05$). Compared with the control, HFD induction increased the proportion of *Firmicutes* but reduced the proportion of *Bacteroidetes* and *Lactobacillus*. *K. marxianus* JLU-1016 and AR strain JLU-1016A treatments improved gut microbiota by reducing the proportion of *Firmicutes* and increasing the proportion of *Bacteroidetes* and *Lactobacillus* in the KI model ($P < 0.0001$). *Helicobacter* has been identified with many infectious diseases and was increased after HFD induction and inhibited after *K. marxianus* JLU-1016 and AR strain JLU-1016A treatments. The strain JLU-1016A exhibited better results possibly with acid-tolerance properties to pass through an acidic environment of the stomach. *Conclusions*. *K. marxianus* may have a beneficial effect on KI by improving gut microbiota and inhibiting TLR4/NF-κB pathway activation.

1. Introduction

High-fat diet (HFD) often results in the incidence of chronic kidney disease (CHD), which may be associated with the changes of gut microbiota [1] and induction of oxidative stress and inflammation [2]. Regulation of gut microbiota may be an effective approach to prevent the progression and development of CHD. Although public health has been paid much attention to the relationship between gut microbiota and kidney injury (KI) [3, 4], there is no effective way approved for kidney disease yet.

Kluyveromyces marxianus exhibits potential probiotic characters by improving immune response and human gut microbiota in an in vitro colonic model system [5]. Oral intake of *K. marxianus* and *Lactobacillus* species was found to mitigate symptoms by reducing the cases of gastrointestinal pyrosis and abdominal pain and musculoskeletal pain in COVID-19 patients [6]. The fermented milk containing *K. marxianus* and *Bifidobacterium lactis* alleviated symptoms (abdominal pain, bloating, and bowel movement disturbances) in irritable bowel syndrome (IBS) patients [7]. *K. marxianus* exerts anti-inflammatory properties, regulates

cellular oxidative stress, and protects the nematodes from oxidative stress by affecting the transcription factor skinhead-1 (SKN-1) via the DAF-2 (dauer formation protein 2, an insulin-like receptor modulating lifespan and stress resistance) [8]. Antioxidant peptides from *K. marxianus* have the highest 2,2-diphenyl-1-picrylhydrazyl (DPPH) radical, 2,2′-azinobis-(3-ethylbenzothiazoline-6-sulfonic acid) (ABTS) radical cation scavenging and ferric reducing capacities, which has a function of cytoprotective properties against Caco2 cells under H_2O_2-modulated oxidative stress by activating the Kelch-like ECH-associated protein 1-nuclear factor erythroid 2-related factor 2 (Keap1-Nrf2) signaling pathway and increasing the activity of antioxidants, such as catalase (CAT), superoxide dismutase (SOD), and glutathione peroxidase (GPX) [9]. The cell wall fractions of *K. marxianus* have antioxidant and immunostimulatory properties [10]. However, the effects of *K. marxianus* on KI and the related molecular mechanism remain unclear.

Toll-like receptor 4 (TLR4) belongs to the family of pattern recognition receptors (PRRs) and plays an important role in the host-innate immune system associated with the inflammatory response via autophagy and oxidative stress [11]. Myeloid differentiation factor 88 (NF-κB), which is an indispensable adaptor molecule for most TLRs, induces the production of inflammatory cytokines via nuclear factor κB (NF-κB) [12], and whose signaling is related to the inflammatory response of KI [13]. TLR4/NF-κB signaling plays a crucial role in inflammation development of KI, and the regulation of the pathway will be beneficial to reduce KI [14, 15]. Alpha inhibitor of NF-κB (IκBα) is the member of the IκB family which binds to NF-κB dimers and sterically blocks its function [16] and shows protective function for KI [17]. Given that TLR4/NF-κB signaling is a chief regulator of inflammation in KI development, its inhibition may be an effective approach to control KI progression. Gastric acidity varies with pH normally between 1.5 and 3.5 and inhibits the viability of probiotics. Acid-resistant (AR) probiotics have more chances to pass through stomach with certain activities when compared with non-acid-resistant strains [18]. The pH of 0.25 M of acetic acid is 2.67, and *K. marxianus* CICC 1727-5 can grow well in the medium with 0.25 M acetic acid [19]. Fortunately, we isolated a strain of *K. marxianus* which can grow well in the medium with pH 2.0. Herein, we used HFD-induced KI mouse model to test the hypothesis that *K. marxianus* or AR strain (which has better acid resistance to pass through stomach) contributes to the protective renal function in the KI model.

2. Materials and Methods

2.1. Animal Grouping. Thirty-two C57BL/6J male mice (4-5 weeks, 18-22 g, $n = 8$ for each group) were purchased from the animal center (China-Japan Union Hospital of Jilin University, Changchun, China) and housed in a light/dark cycle (12/12 h). After a one-week acclimatization period, the animals were fed with HFD diet (20% protein (casein and methionine), 36% fat (lard), 4% ash, <5% moisture, 34% carbohydrate (maltodextrin and sucrose), 2.5% minerals and vitamin mix, and 60% calories from fat; Research Diets, Xietong Biotechnology Company, Nanjing, China) for 4 weeks to induce KI. Low-fat diet (20% protein (casein and methionine), 6% fat (lard), 4% ash, <5% moisture, 64% carbohydrate (maltodextrin, cornstarch, and sucrose), 2.5% minerals and vitamin mix, and 14% calories from fat) was used as a control. All *K. marxianus* strains were resuspended with saline (pH = 7.0) before administration. Then, the mice were evenly divided into four groups, and the mice were orally administered with *K. marxianus* JLU-1016 (0.5×10^8 to 1×10^8 cells/mL in saline solution, 0.5 mL/day; the strain grew in the YPD medium with pH 7.0, MG group) or equal volume of AR *K. marxianus* JLU-1016A (0.5×10^8 to 1×10^8 yeast cells/mL in saline solution, 0.5 mL/day; the strain grew in the YPD medium with pH 2.0, AG group) for 4 weeks. The other two groups received saline as the normal control (CG) and HFD-induced group (HG) (Figure 1). After the experiment, body weight was measured. In the end, the mice were fasted for 8 h, anesthetized using isoflurane, and sacrificed to obtain blood and tissues. Other experiments were performed as Figure 1 showed. All experiments were approved by the Animal Research Ethics Committees of China-Japan Union Hospital of Jilin University.

2.2. Oral Glucose Tolerance Test (OGTT). We performed glucose tolerance tests after 4-week oral administration of the probiotics (Figure 1). The mice were fasted overnight and then orally administered with D-glucose by gavage (2 g/kg, $n = 3$ for each group) [20, 21], which was dissolved in 20 mM PBS (10% D-glucose, pH 7.0). Blood glucose levels were measured by using a blood glucose meter (Yicheng, Beijing, China). Blood glucose was measured from the tail vein at 0, 15, 30, 60, 90, and 120 min after the oral load of glucose. The area under the ROC curve (AUC) of OGTT was plotted by using GraphPad Prism.

2.3. Hematoxylin and Eosin (H&E) Staining of KI Tissues. KI tissues were fixed in 4% formalin solution for fixation. Subsequently, the tissues were dehydrated, immersed in wax, embedded in paraffin to prepare four μm paraffin sections, and collected on slides and processed according to a previous report [22]. The pathological changes of KI were confirmed under a light microscope. Histopathology scoring was used according to the reported standard [22]. The average scores were calculated by randomly selecting five different eye fields, which reflected tubular necrosis, cast formation, lack of brush border, and tubular dilatation follows: 1 (less than 10%), 2 (11-25%), 3 (26-45%), 4 (46-75%), and 5 (more than 75%).

2.4. Terminal Deoxynucleotidyl Transferase (TdT) dUTP Nick End Labeling (TUNEL) Assay. The apoptosis index of KI tissues was analyzed by using TUNEL Cell Apoptosis Detection Kit (Cat. No. C1091, Beyotime, China). Five random fields of view for each KI tissue were observed under an inverted Olympus microscope with an original magnification ×200 (Olympus, Tokyo, Japan). The amounts of TUNEL-positive cells were calculated by using ImageJ software (NIH, Bethesda, MD, USA). Apoptotic rate = 100

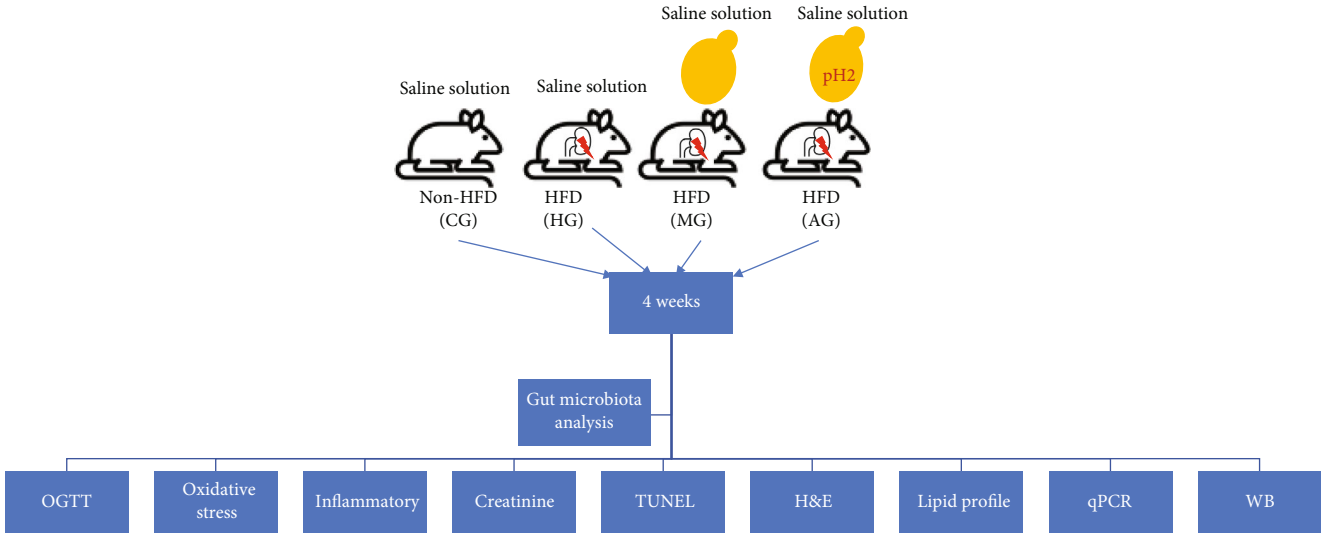

Figure 1: The flow chart of this study. $n = 8$ for each group.

× (the amounts of TUNEL – positive cells/total number of cell present).

2.5. Lipid Profile Analysis. Zero point three mL of blood was obtained from each mouse by heart puncture, and serum was isolated via a centrifuge (2000 g, 15 min, and 4°C). Serum triglycerides (TG), total cholesterol (TC), high-density lipoprotein cholesterol (HDL-c), and low-density lipoprotein cholesterol (LDL-c) were measured spectrophotometrically by using the kits from Ruixin Biotechnology Company (Quanzhou, China).

2.6. Measurement of Oxidative Stress Marker. Zero point three mL of blood was obtained from each mouse by heart puncture, and serum was isolated via a centrifuge (2000 g, 15 min, and 4°C). The indexes of serum SOD, serum glutathione (GSH), and serum lipid peroxidation marker malondialdehyde (MDA) were measured using the assay kit from Ruixin Biotechnology Company (Quanzhou, China) according to the manufacturer's instructions.

2.7. Measurement of Inflammatory Cytokines. Fifty mg kidney was obtained and grounded with a glass homogenizer in 1 mL of PHB buffer (20 mM, 50 mM NaCl, and a cocktail of proteinase inhibitors, pH 7.0). The mixture was centrifuged at 10,000 g for 10 min at 4°C, and supernatant was collected. The indexes of IL-1β, IL-6, and TNF-α were measured using the assay kit from Ruixin Biotechnology Company (Quanzhou, China) according to the manufacturer's instructions.

2.8. Measurement of Urine and Serum Creatinine. Twenty-four-hour urine samples were collected by using metabolic cages at the end of 4-week treatment. Urine and serum creatinine were measured by using a Mouse Albumin ELISA quantitation kit (Cat. No. D799853-0096, Shanghai Sangon Biological Engineering Technology and Services Company Ltd., Shanghai, China).

2.9. qPCR. The total RNA from kidney tissue was extracted with a TRIzol extraction kit (Cat. No. B511311-0025, Shanghai Sangon Biological Engineering Technology and Services Company Ltd., Shanghai, China). The reverse transcription was performed with the BeyoRT™ II cDNA Synthesis Kit (Cat. No. D7170M, Beyotime Biotechnology Company, Shanghai, China). Quantitative assay of gene expressions was carried out by using BeyoFast™ SYBR Green qPCR Mix (Cat. No. D7260, Beyotime Biotechnology Company, Shanghai, China) and a CFX96 Touch real-time PCR system (Bio-Rad, Hercules, CA, USA). The gene expression was normalized to the GAPDH and analyzed via the $2^{-\Delta\Delta CT}$ method. The primers of GAPDH, Toll-like receptor 4 (TLR4), nuclear factor kappa B (NF-κB), and alpha inhibitor of NF-κB (IκBα) were synthesized according to the previous reports [23–26].

2.10. Western Blot. After the isolation of kidney issues, 50 mg of tissues was obtained and grounded with a glass homogenizer in 1 mL of PHB buffer (20 mM, 50 mM NaCl, and a cocktail of proteinase inhibitors, pH 7.0). Protein was isolated by using the cell membrane protein and cytoplasmic protein extraction kit (Cat. No. P0033, Beyotime Biotechnology Company, Shanghai, China). The protein concentration was determined using a bicinchoninic acid (BCA) assay via the Protein Concentration Assay Kit (Cat. No. P0010, Beyotime Biotechnology Company, Shanghai, China) before SDS-PAGE and Western blot studies. Twenty to 40 μg protein was separated using 12% SDS-PAGE and transferred to the polyvinylidene fluoride membranes, which were incubated with 100 μL primary antibodies for anti-TLR4 mAb (1 : 1000, Cat. No. 66350-1-Ig, Proteintech, Wuhan, China), anti-IκBα mAb (1 : 1000, Cat. No. 10268-1-AP, Proteintech, Wuhan, China), rabbit anti-phospho-NF-κB p65 (Ser536) (1 : 1000, Cat. No. AN371, Beyotime Biotechnology, Beijing, China), and anti-GAPDH polyclonal antibody (1 : 1000, Cat. No. 10494-1-AP, Proteintech, Wuhan, China) in Tris–HCl buffer saline with 5% BSA at 4°C overnight and followed

by incubation with 100 μL horseradish enzyme-labeled goat antirabbit IgG (1 : 2000, Cat. No. D110058-0100, Shanghai Sangon Biological Engineering Technology and Services Company Ltd., Shanghai, China) or horseradish enzyme-labeled goat antimouse IgG (1 : 2000, Cat. No. SPA131, Solebol, Beijing, China). The intensity of protein bands was quantified using Bio-Rad ChemiDoc XRS+ Imaging System (Bio-Rad, Hercules, CA, USA).

2.11. Gut Microbiota Analysis. For gut microbiota analysis, the feces of mice were collected in a sterile two-mL-tube and stored in a -80°C freezer until next step. DNA was isolated and purified from the feces using the UNIQ-10 Spin kit (Shenggong Biotechnology Co., Ltd., Shanghai, China). Thermal cycling was carried out with the CFX 96 Real-Time system (Bio-Rad) by using DNA polymerase (Shenggong Biotechnology Co., Ltd., Shanghai, China) with the following reaction conditions: initial denaturation at 95°C for 4 min; 10 cycles of denaturation at 95°C for 30 s, annealing at 50°C for 30 s, and extension at 72°C for 30 s; final extension at 72°C for 5 min. The amplified PCR products were purified by using the UNIQ-10 PCR-clean-up kit (Shenggong Biotechnology Co., Ltd., Shanghai, China). The quality of PCR production was evaluated by using a Bioanalyzer 2100 (Agilent, Palo Alto, Ca, USA) via a DNA 7500 chip. The amplicons were collected for sequencing by using Illumina MiSeq PE300 platform (Illumina, USA). The PE reads obtained by next-generation sequencing were firstly spliced according to the overlap relationship, and the sequence quality was controlled and filtered after the samples were distinguished, and then, OTU clustering analysis and taxonomic analysis were performed. Based on OTU clustering analysis results, OTU was analyzed for diversity index and sequencing depth detection; based on taxonomic information, statistical analysis of community structure was performed at each taxonomic level. Beta diversity was used to compare the diversity among different groups and was used to express the response of gut microbiota to environmental heterogeneity. To assess alpha diversity, Shannon's index was used to calculate community evenness, Chao1 was used for genus richness, and Simpson's diversity index was used to evaluate the number of genus and the relative abundance of each genus. Alpha diversity and beta diversity were analyzed by using microbiome R package [27], dplyr R package [28], and vegan R package [29]. Rank abundance curve was plotted by using Biodiversity R package [30] to reflect relative genus abundance, richness, and evenness. Venn diagram was plotted by using VennDiagram R package [31] to show the number of exclusive and shared genus among different groups. Circos collinearity was plotted by using RCircos package [32] and circlize R package [33] to compare the shared genus distribution in different groups. The dendrogram of the taxonomic system of all groups was plotted, and function was analyzed by using phyloseq R package [34].

2.12. Statistical Analysis. All values were showed as mean ± standard deviation (S.D.). Statistical analysis was carried out via GraphPad Prism, and $P < 0.05$ was considered significant. A Student's t-test was used to compare the differences between the two groups, and analysis of variance (ANOVA) was used to compare the statistical significance among different groups. Each experiment was performed triplicated.

3. Results

3.1. K. Marxianus Prevented Weight Gain and Improved Glucose Tolerance of the Mice. The weight of the mice in the HG group increased significantly when compared to the CG group (Figure 2(a), $P < 0.0001$) after 4-week model establishment. After 4-week *K. marxianus* treatment, the weight was significantly reduced when compared with the mice from the HG group, and AR strain JLU-1016A reduces the weight more than the wild one (Figure 2(a), $P < 0.0001$ vs. $P < 0.001$). During the OGTT test, blood glucose levels in the HG group were significantly higher than the CG group (Figure 2(b), $P < 0.01$). However, *K. marxianus* JLU-1016 and AR strain JLU-1016A treatments did not cause a significant decrease in blood glucose (Figure 2(b), $P > 0.05$). AUC analysis of OGTT showed that there was significant discrimination between the CG and HG groups (AUC = 0.76), but weak discrimination between the MG or AG and HG groups (AUC = 0.60 for both) (Figure 2(c)). Taken together, these data showed that *K. marxianus* treatment reduces the mouse weight but cannot improve glucose tolerance in the HFD-challenged mice yet.

3.2. K. Marxianus Alleviated HFD-Induced KI. At the end of the experiment, HFD diet induced the thickened glomerular basement membrane, and vacuolated tubules and glomerulomegaly were considerably created in the mouse model when compared with the CG group (Figure 3(a)). The damaged morphology was remarkably improved in the mouse model after *K. marxianus* JLU-1016 or AR strain JLU-1016A treatment (Figure 3(a)). HFD induction increased the H&E staining scores when compared to those in the CG group (Figure 3(b), $P < 0.0001$). *K. marxianus* JLU-1016 or AR strain JLU-1016A treatment reduced the scores in the model, and latter strain showed more reduction in the scores (Figure 3(b), $P < 0.01$ vs. $P < 0.001$).

3.3. K. Marxianus Reduced the Apoptotic Rate in HFD-Induced KI Model. HFD diet increased the apoptotic rate in the mouse model when compared with the CG group (Figures 4(a) and 4(b), $P < 0.0001$). The apoptotic rates were reduced in the mouse model after *K. marxianus* JLU-1016 or AR strain JLU-1016A treatment, and the latter strain showed more reduction in the apoptotic rate (Figures 4(a) and 4(b), $P < 0.001$ vs. $P < 0.001$). The results suggest that *K. marxianus* can control the apoptosis in the mouse model while the AR strain JLU-1016A shows better results.

3.4. K. Marxianus Improved the Lipid Profile in HFD-Induced KI Model. HFD diet increased the levels of TG, TC, and LDL-c and reduced HDL-c in the mouse model when compared with the CG group (Figure 5(a), $P < 0.0001$; Figure 5(b), $P < 0.01$; Figure 5(c), $P < 0.0001$; Figure 5(d), $P < 0.05$). The levels of TG, TC, and LDL-c were reduced, and the level of HDL-c was increased after *K.*

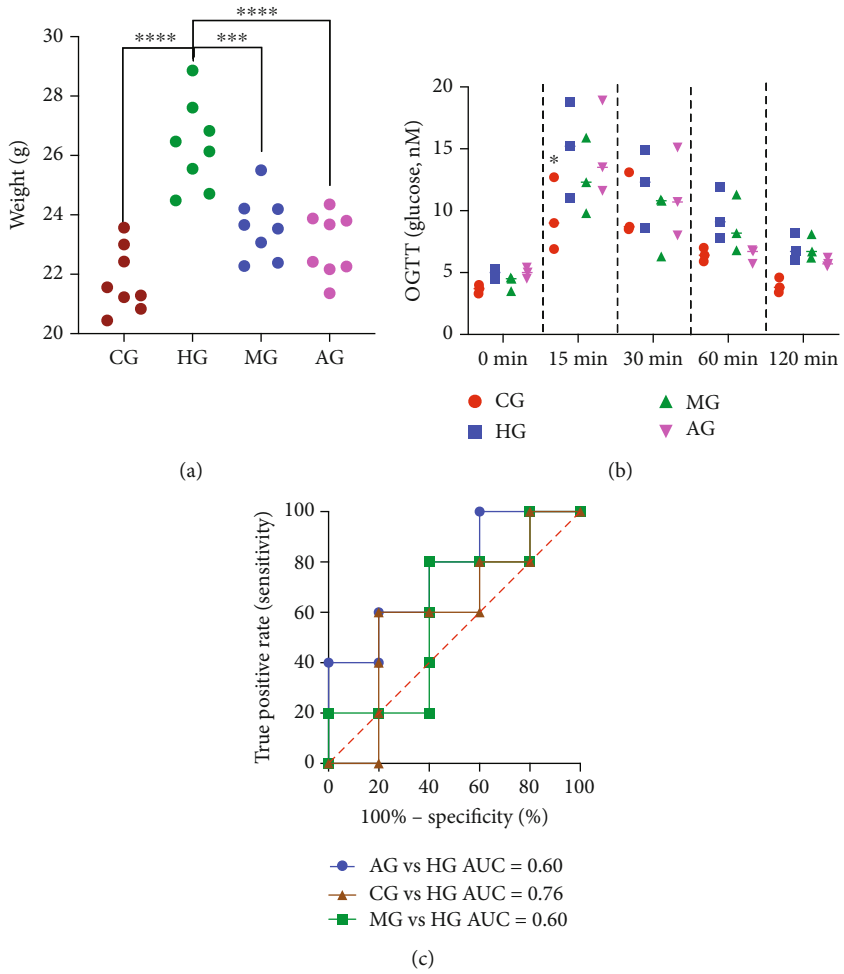

Figure 2: The effects of *Kluyveromyces marxianus* on mouse weight and glucose tolerance. (a) The weight of the mice. $n = 8$ for each group. (b) An oral glucose tolerance test (OGTT) for glucose tolerance. $n = 3$ for each group. (c) The area under the ROC curve (AUC) of OGTT. $^{**}P < 0.01$, $^{***}P < 0.001$, and $^{****}P < 0.0001$ vs. the HG group.

marxianus JLU-1016 or AR strain JLU-1016A treatment (Figure 5(a), $P < 0.0001$ for both; Figure 5(b), $P > 0.05$ and $P < 0.01$; Figure 5(c), $P < 0.001$ for lower vs. $P < 0.0001$ for higher; Figure 5(d), $P < 0.05$ and $P < 0.01$). The results suggest that *K. marxianus* can improve the lipid profile, and AR strain JLU-1016A showed better results.

3.5. K. Marxianus Improved Antioxidant Properties in HFD-Induced KI Model. HFD diet reduced the activities of serum SOD (Figure 6(a), $P < 0.01$) and serum GSH (Figure 6(b), $P < 0.0001$) but no changes in the concentration of serum MDA (Figure 6(c), $P > 0.05$). *K. marxianus* JLU-1016 increased the activities of serum SOD (Figure 6(a), $P < 0.01$) but no change for serum GSH (Figure 6(b), $P > 0.05$) and the concentration of serum MDA (Figure 6(c), $P > 0.05$). The AR *K. marxianus* JLU-1016A increased the activities of serum SOD (Figure 6(a), $P < 0.01$) and serum GSH (Figure 6(b), $P < 0.001$), and no change for the concentration of serum MDA (Figure 6(c), $P > 0.05$). The results suggest that *K. marxianus* improves antioxidant properties in the KI model.

3.6. K. Marxianus Improved the Anti-Inflammatory Properties in the KI Model. HFD diet increased the levels of kidney IL-1β (Figure 7(a), $P < 0.01$), kidney IL-6 (Figure 7(b), $P < 0.0001$), and kidney TNF-α (Figure 7(c), $P < 0.0001$) when compared with the CG group. In contrast, *K. marxianus* JLU-1016 and AR strain JLU-1016A treatments reduced the levels of kidney IL-1β (Figure 7(a), $P < 0.0001$), kidney IL-6 (Figure 7(b), $P < 0.0001$), and kidney TNF-α (Figure 7(c), $P < 0.001$). The results suggest that *K. marxianus* improves the anti-inflammatory properties in the KI model by reducing the levels of kidney IL-1β, IL-6, and TNF-α.

3.7. Acid-Resistant K. Marxianus Reduced Creatinine Levels in the KI Model. HFD diet increased the levels of urine creatinine (Figure 8(a), $P < 0.001$) and serum creatinine (Figure 8(b), $P < 0.05$) when compared with the CG group. In contrast, *K. marxianus* JLU-1016 treatment did not change the levels of urine creatinine (Figure 8(a), $P > 0.05$) and serum creatinine (Figure 8(b), $P > 0.05$) when compared with the HG group. The AR strain JLU-1016A reduced the

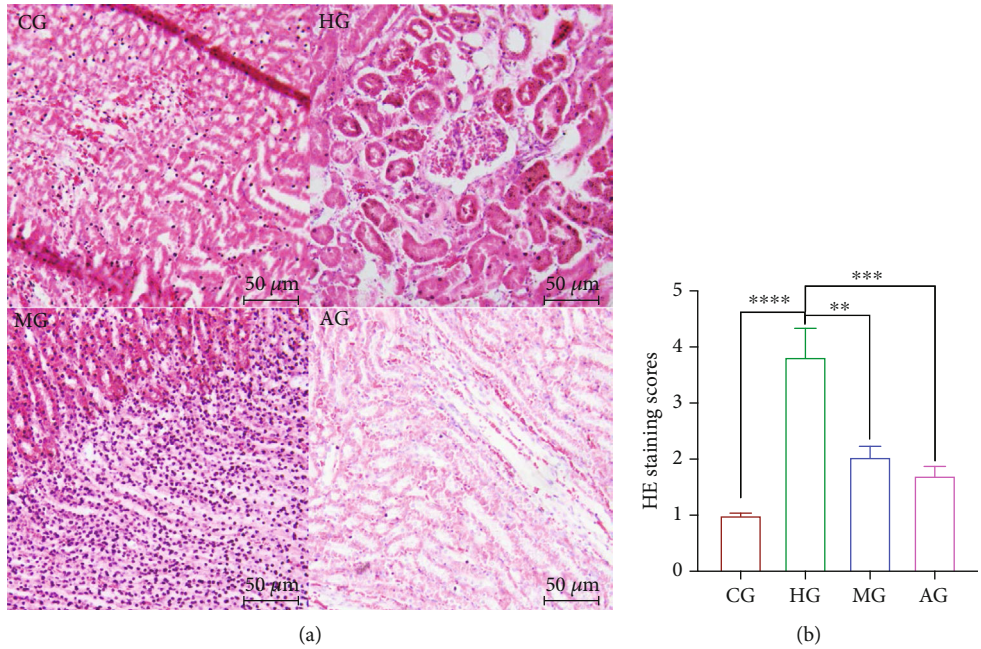

Figure 3: Hematoxylin and Eosin (H&E) staining of the kidney injury. (a) H&E-stained glomeruli or renal tubules. (b) H&E-stained histological scores. Magnification: 100x; scale bar: 50 μm. $n = 3$ for each group, and $^{**}P < 0.01$, $^{***}P < 0.001$, and $^{****}P < 0.0001$ vs. the HG group.

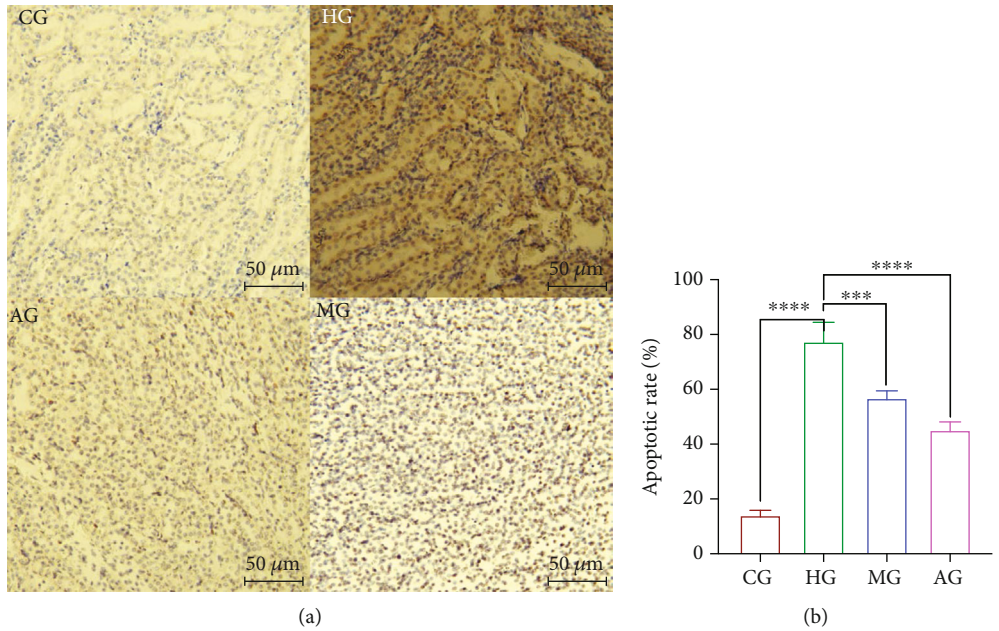

Figure 4: Terminal deoxynucleotidyl transferase dUTP nick end labeling (TUNEL) analysis of apoptotic cells in kidney tissue. (a) The imaging results using TUNEL Cell Apoptosis Detection Kit. (b) Apoptotic rate measured by the percent of TUNEL-positive cells. Magnification: 100x; scale bar: 50 μm. $n = 3$ for each group, and $^{***}P < 0.001$ and $^{****}P < 0.0001$ vs. the HG group.

levels of urine creatinine (Figure 8(a), $P < 0.001$) and serum creatinine (Figure 8(b), $P < 0.01$) when compared with the HG group. The results suggest that AR strain JLU-1016A can improve the creatinine levels but not for the non-acid-resistant strain JLU-1016.

3.8. K. Marxianus Reduced TLR4, NF-κB, and IκBα Levels in HFD-Induced KI Model. HFD diet increased the relative mRNA levels of TLR4 (Figure 9(a), $P < 0.0001$) and NF-κB (Figure 9(b), $P < 0.0001$) and reduced IκBα (Figure 9(c), $P < 0.05$) when compared with those molecules in the CG

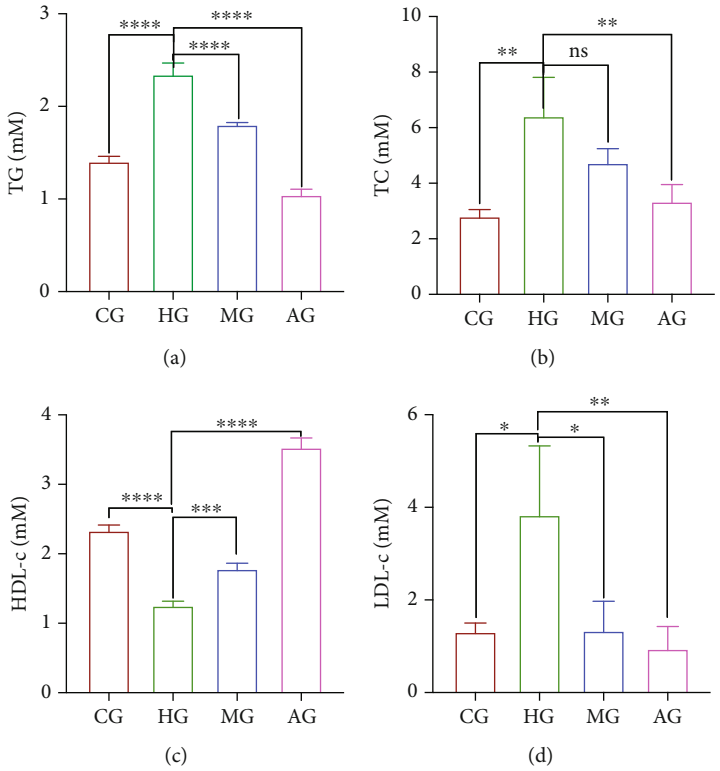

Figure 5: The effects of *Kluyveromyces marxianus* on lipid profiles. (a) TG. (b) TC. (c) HDL-c. (d) LDL-c. $n = 3$ for each group, and $^{ns}P > 0.05$, $^{*}P < 0.05$, $^{**}P < 0.01$, $^{***}P < 0.001$, and $^{****}P < 0.0001$ vs. the HG group.

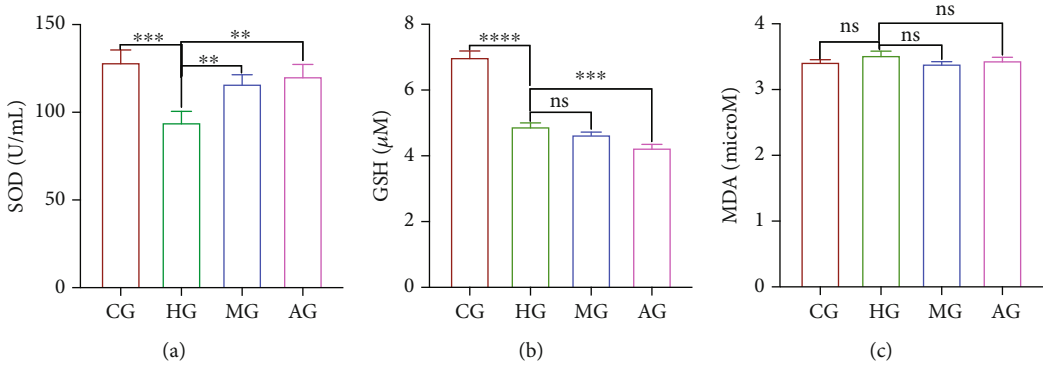

Figure 6: The levels of oxidative factors. (a) Serum SOD. (b) Serum GSH. (c) Serum MDA. $n = 3$ for each group, and $^{ns}P > 0.05$, $^{**}P < 0.01$, $^{***}P < 0.001$, and $^{****}P < 0.0001$ vs. the HG group.

group. In contrast, *K. marxianus* JLU-1016 and AR strain JLU-1016A treatments reduced the relative mRNA levels of TLR4 (Figure 9(a), $P < 0.0001$) and NF-κB (Figure 9(b), $P < 0.001$) and increased IκBα (Figure 9(c), $P < 0.001$) when compared with those molecules in the HG group. Similarly, HFD diet increased the relative protein levels of TLR4 (Figures 9(d) and 9(e), $P < 0.0001$) and NF-κB (Figures 9(d) and 9(f), $P < 0.0001$) and reduced IκBα (Figures 9(d) and 9(g), $P < 0.0001$) when compared with those molecules in the CG group. In contrast, *K. marxianus* JLU-1016 and AR strain JLU-1016A treatments reduced the relative protein levels of TLR4 (Figures 9(d), and 9(e) $P < 0.0001$) and NF-κB (Figures 9(d) and 9(f), $P < 0.0001$) and increased IκBα (Figures 9(d) and 9(g), $P < 0.001$) when compared with those molecules in the HG group. The results suggest that *K. marxianus* treatments affect TLR4/NF-κB inflammatory signaling in the KI model.

3.9. K. Marxianus Treatment Affected the Gut Microbiota in HFD-Induced KI Model. Shannon's diversity index shows the overall community heterogeneity and genus richness. HFD diet reduced the richness and evenness of gut microbiota when compared with the CG group (Figure 10(a), $P < 0.0001$). *K. marxianus* JLU-1016 and the AR strain JLU-1016A treatments did not increase the richness and evenness

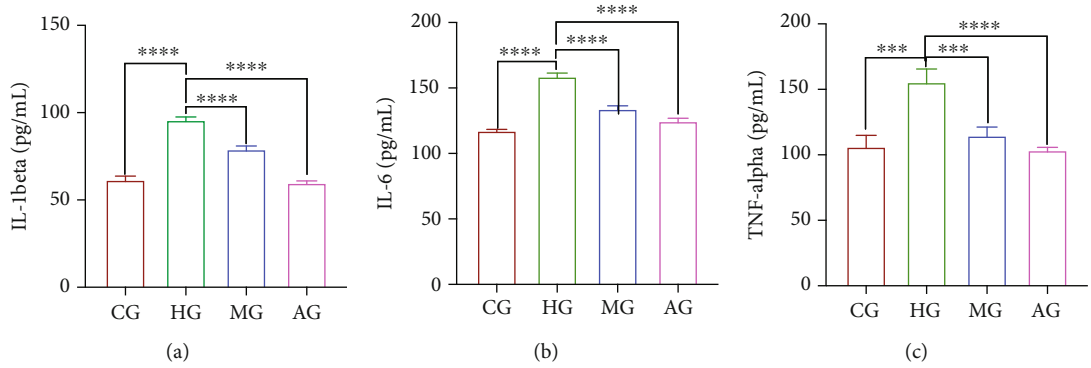

Figure 7: The levels of inflammatory cytokines. (a) IL-1β. (b) IL-6. (c) TNF-α. $n = 3$ for each group, and $^{ns}P > 0.05$ and $^{****}P < 0.0001$ vs. the HG group.

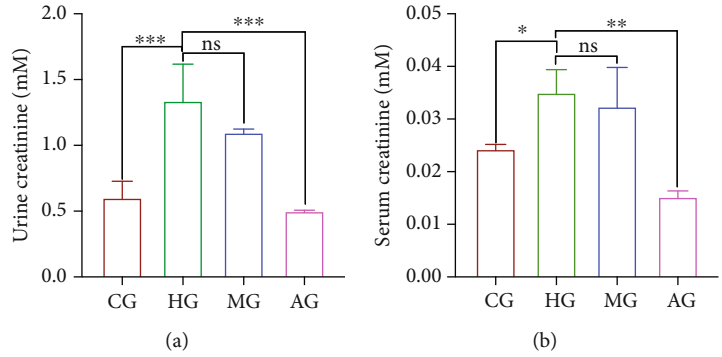

Figure 8: The levels of urine and serum creatinine. (a) The concentration of urine creatinine. (b) The concentration of serum creatinine. $n = 3$ for each group, and $^{ns}P > 0.05$, $^{*}P < 0.05$, $^{**}P < 0.01$, and $^{***}P < 0.001$ vs. the HG group.

of gut microbiota when compared with the HG group (Figure 10(a), $P > 0.05$). Chao1 index shows the genus richness. HFD diet reduced the genus richness of gut microbiota when compared with the CG group (Figure 10(b), $P < 0.01$). On the other hand, the AR strain JLU-1016A treatments but not non-acid-resistant *K. marxianus* increased the genus richness of gut microbiota when compared with the HG group (Figure 10(b), $P < 0.01$). Simpson's diversity index is used to evaluate the number of genus and the relative abundance of each genus, both of which increase and the diversity will increase. HFD diet reduced the diversity of gut microbiota when compared with the CG group (Figure 10(c), $P < 0.0001$). On the other hand, the AR strain JLU-1016A treatments but not non-acid-resistant *K. marxianus* JLU-1016 increased the diversity of gut microbiota (Figure 10(c), $P < 0.01$). Principal coordinate analysis (PCoA) based on Bray-Curtis (Figure 10(d)) and Jaccard (Figure 10(e)) distances demonstrated that the overall gut microbiota structures of the HG group were distinct from the CG, AG, and MG groups with AG clustering closer to the CG group. PCoA also showed small fraction of the total variance between Bray-Curtis (Figure 10(d)) and Jaccard (Figure 10(e)) distances. The rank abundance curve shows the gut microbiota diversity and dominance patterns. HFD diet reduced the diversity of gut microbiota and the dominance pattern when compared with the CG group (Figure 10(f), $P < 0.0001$). On the other hand, *K. marxianus* JLU-1016 and AR strain JLU-1016A treatments increased gut microbiota diversity and the dominance genus when compared with HG group (Figure 10(f), $P < 0.0001$). Venn diagram showed the similar changing trend for the species diversity (HG, 211 species; CG, 260 species; MG, 237 species; AG, 258 species) with the results analyzed by rank abundance curve (Figures 10(f) and 10(g)). Circos collinearity plot shows the shared genus distribution among different groups and indicated that *Bacteroidetes* are the dominant genus, and *Firmicutes* are a small fraction of the gut microbiota in the CG group while HFD induction reduced the *Bacteroidetes* significantly and increased the proportion of *Firmicutes* (Figure 10(h)). On the other hand, *K. marxianus* JLU-1016 and AR strain JLU-1016A treatments reduced the proportion of *Firmicutes* but increased the proportion of *Bacteroidetes* when compared with HG group (Figure 10(h), $P < 0.0001$). Furthermore, *Saccharibacteria*, which is an extremely small coccus and not previously observed in human-associated microbes, appeared in the HG, AG, and MG groups. The dendrogram of the taxonomic system showed the genus of all groups at a genus level. *Actinobacteria, Bacteroidetes, Lactobacillus, Barnesiella, Prevotella, Alloprevotella, Olsenella,* and *Parasutterella* are the predominant genera in the CG group. HFD induction reduced the proportion of *Lactobacillus* and *Bacteroidetes* while *K. marxianus* JLU-1016 and AR strain JLU-1016A treatments reversed the reduction in these genera (Figure 10(i)). Many novel *Helicobacter* have been identified with human in many

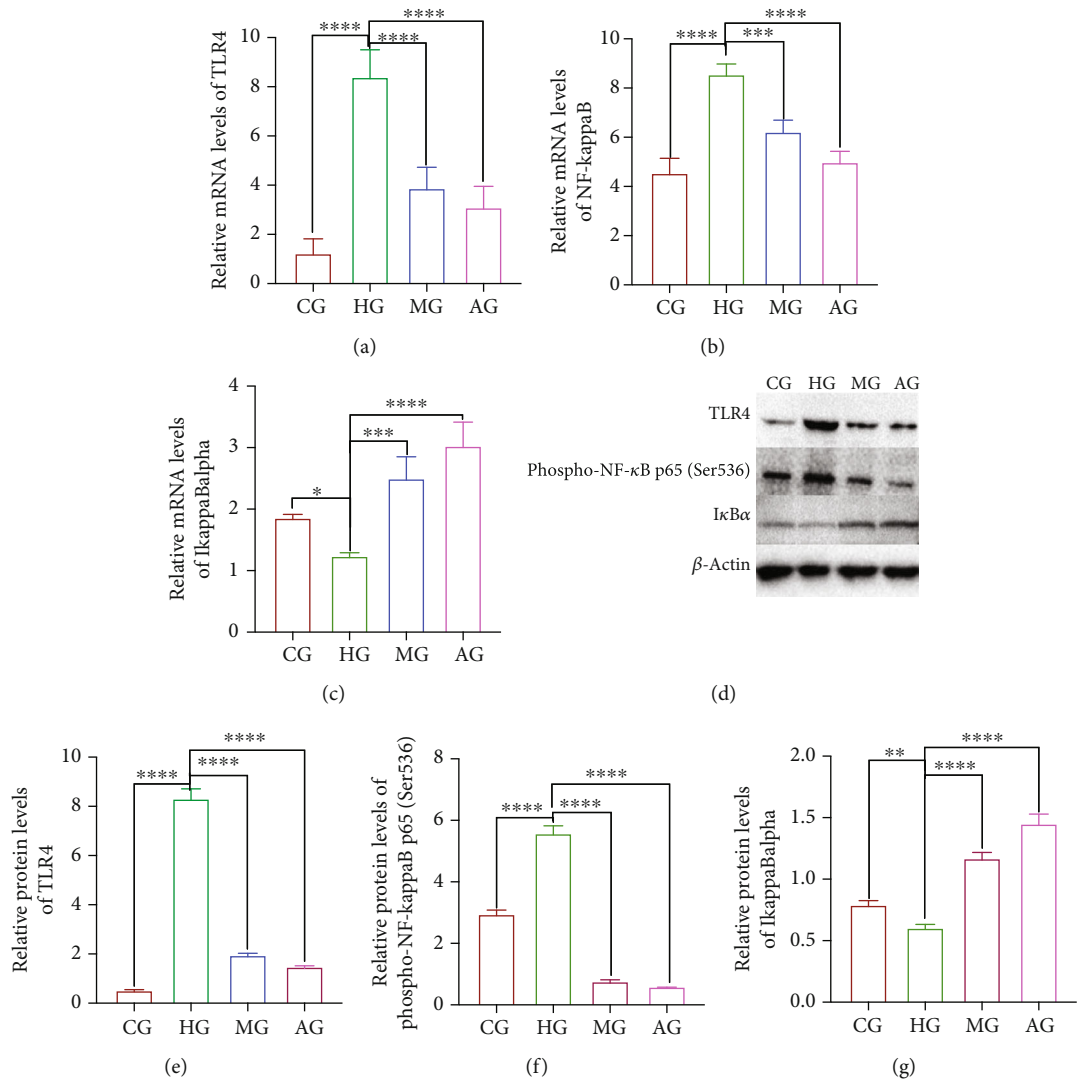

FIGURE 9: The levels of TLR4, NF-κB, and IκBα. (a) Relative mRNA levels of TLR4. (b) Relative mRNA levels of NF-κB. (c) Relative mRNA levels of IκBα. (d) Western Blot. (e) Relative protein levels of TLR4. (f) Relative protein levels of phospho-NF-κB p65 (Ser536). (g) Relative protein levels of κBα. $n = 3$ for each group, and $^{*}P < 0.05$, $^{**}P < 0.01$, $^{***}P < 0.001$, and $^{****}P < 0.0001$ vs. the HG group.

infection diseases [35–37] and are increased in the HG, and the genera were inhibited after *K. marxianus* JLU-1016 and AR strain JLU-1016A treatments (Figure 10(i)). Function analysis showed that HFD induction reduced the levels of the protein involved with multiple sugar transport system, polar amino acid transport system, and peptide transport system and increased the protein involved with antibiotic transport system, beta-galactosidase, and iron complex outer-membrane receptor while *K. marxianus* and the AR strain reversed all these parameters (Figure 10(j)).

4. Discussion

HFD is closely associated with the progression and development of kidney failure [38]. HFD induces obesity associated with gut microbiota and increased body weight [39], which plays an important role in the obesity-related kidney diseases [40, 41]. In this study, HFD induction increased the body weight, apoptotic rate, oxidative stress, creatinine levels, inflammation levels, and expression of the inflammation-related TLR4/NF-κB signaling pathway and reduced the glucose tolerance. *K. marxianus* JLU-1016 and AR strain JLU-1016A treatments improved these parameters except of oxidative stress. Furthermore, HFD induction increased the proportion of *Firmicutes* but reduced the proportion of *Bacteroidetes* and *Lactobacillus*. *K. marxianus* JLU-1016 and AR strain JLU-1016A treatments improved gut microbiota by reducing the proportion of *Firmicutes* and increasing the proportion of *Bacteroidetes* and *Lactobacillus* when compared with the KI model group. *Helicobacter* was increased after HFD induction, and the genus was inhibited after *K. marxianus* and AR strain treatments (Figure 10(g)). HFD induction prevents the expression of the protein responsible for the transport of multiple sugar, polar amino acid, and peptide and increased the protein responsible for antibiotic transport system, beta-galactosidase, and iron complex outer-membrane

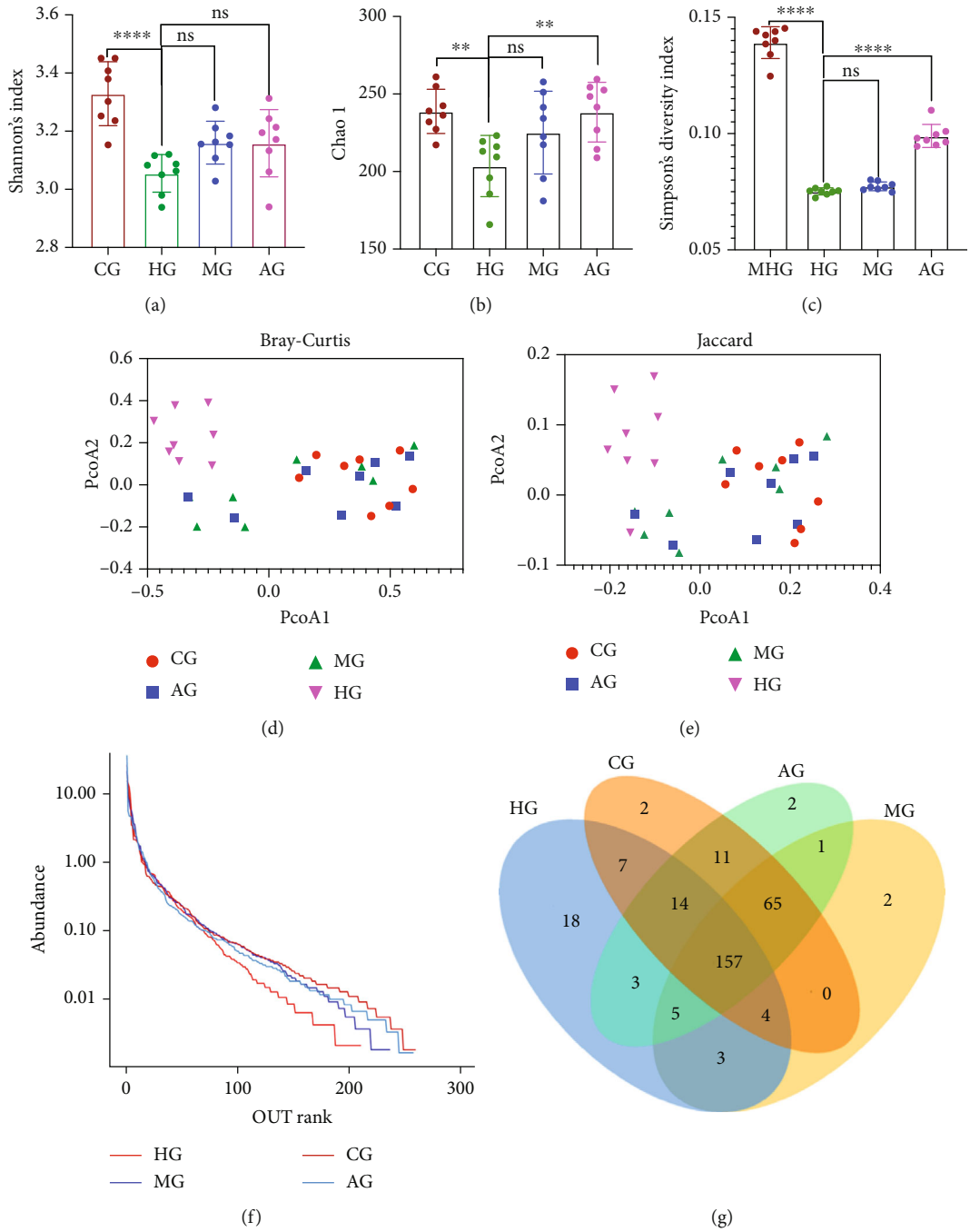

Figure 10: Continued.

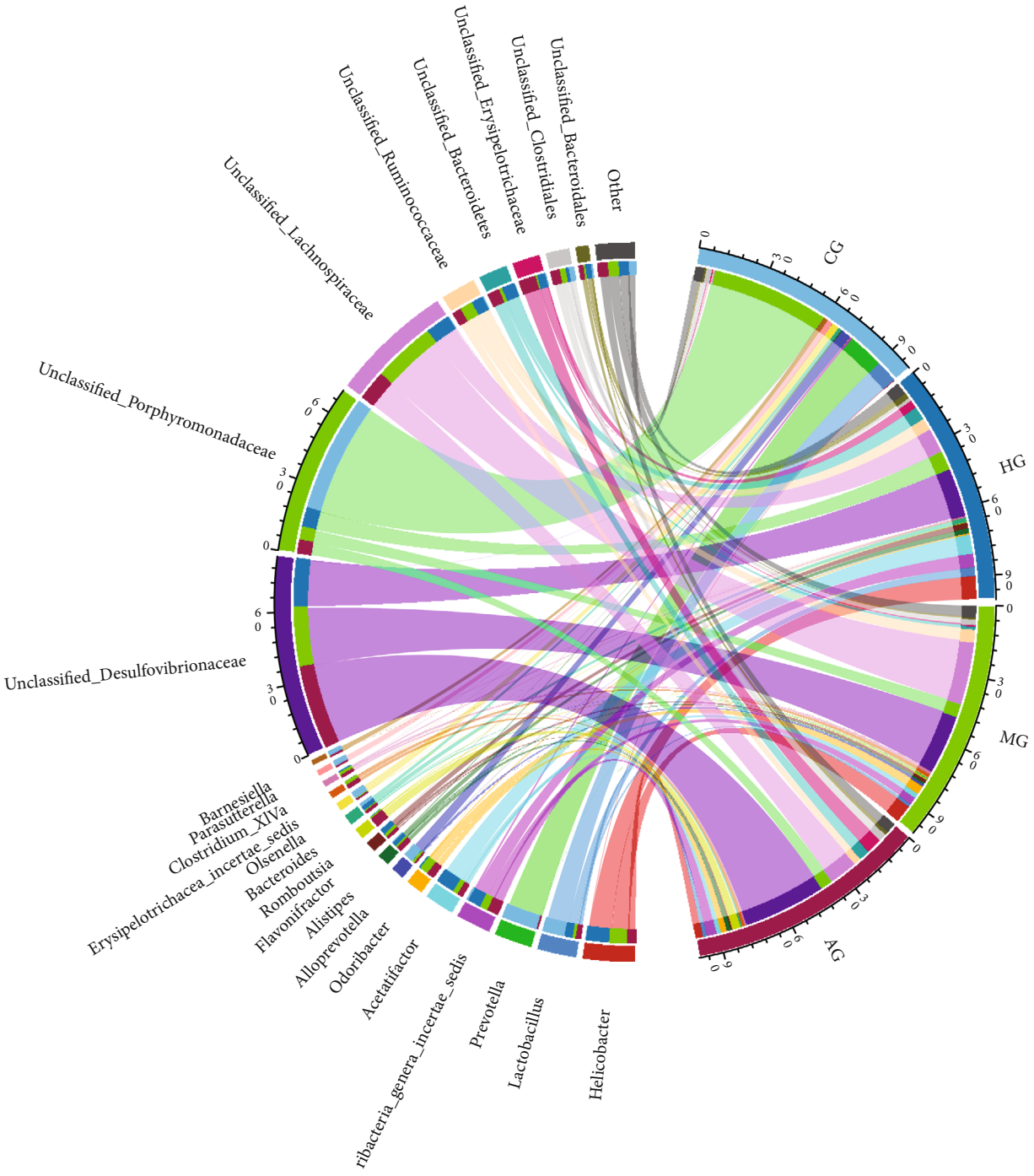

(h)

Figure 10: Continued.

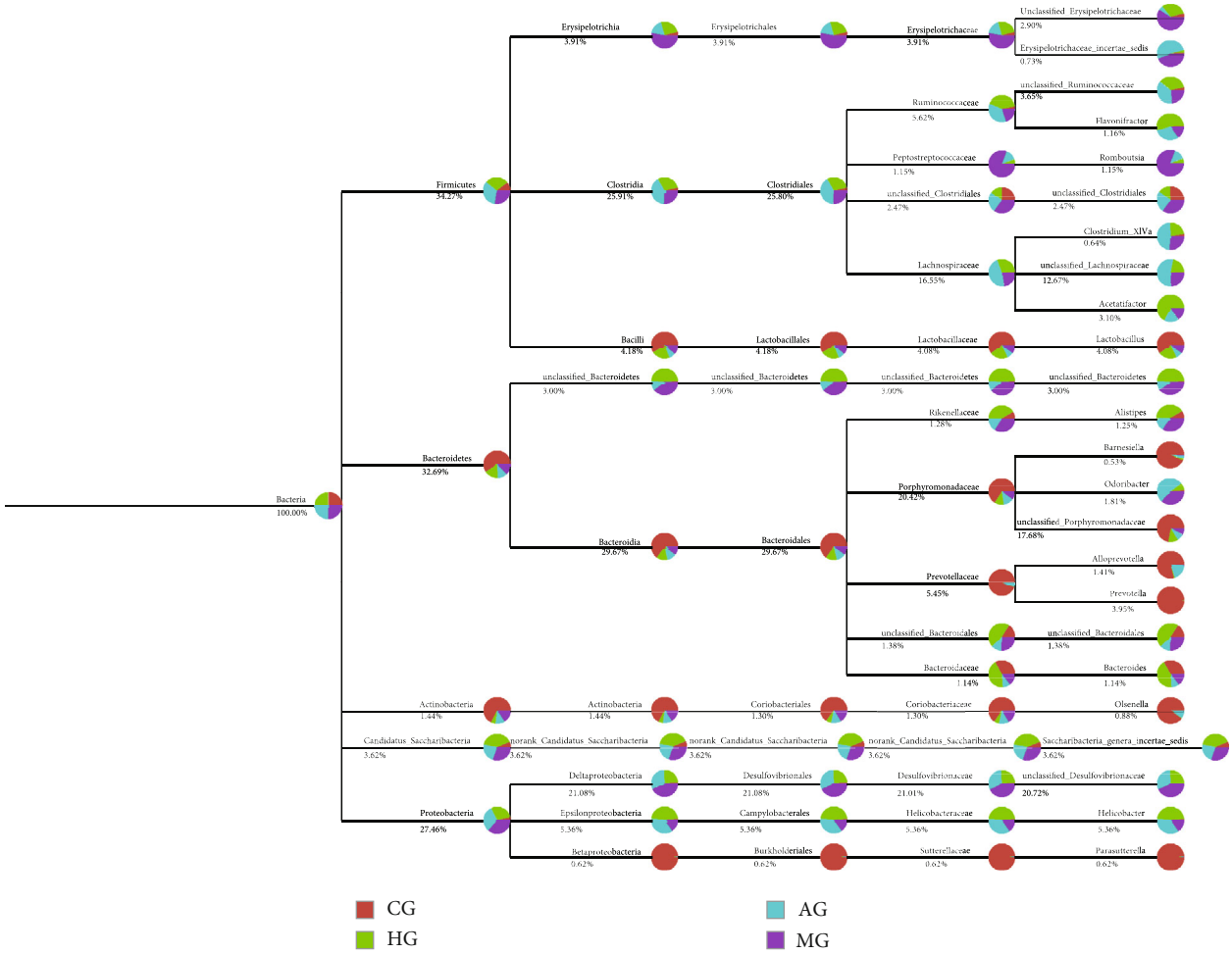

(i)

Figure 10: Continued.

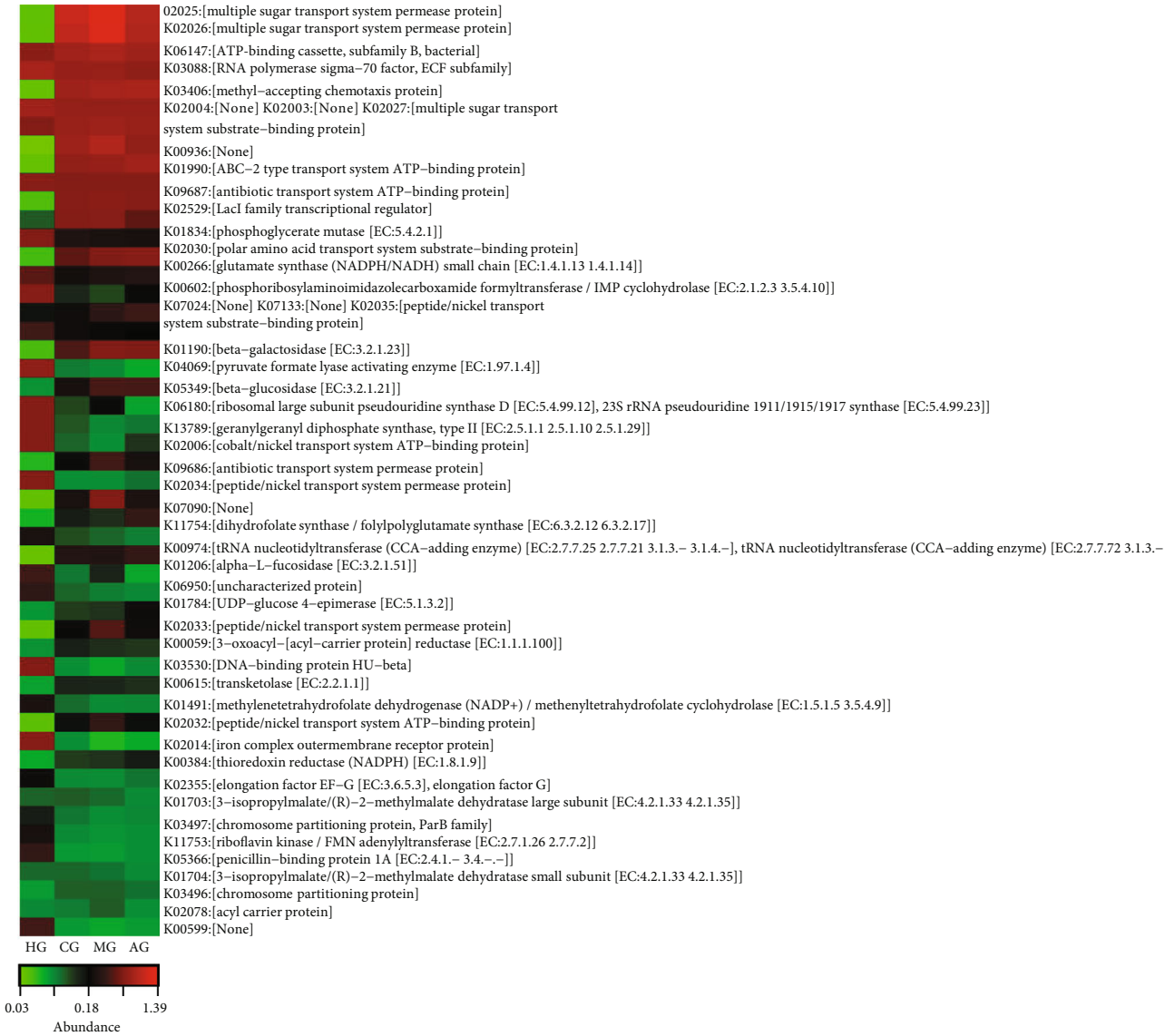

(j)

Figure 10: Diversity analysis of gut microbiota among four groups. (a) Shannon's index. (b) Chao1. (c) Simpson's diversity index. (d) Principal coordinate analysis (PCoA) plotted with Bray-Curtis. (e) PCoA plotted with Jaccard. (f) Rank abundance curve. (g) Venn diagram. (h) Circos collinearity plot. (i) The dendrogram of the taxonomic system of all groups at a genus level. (j) Function analysis. The differences in the abundance of different groups on a branch are compared, which are presented by a colored pie chart. Different colors represent different groups, and the larger the fan-shaped area of the color shows, the higher the abundance of the species in the specific group on the branch. Near the fulcrum are the taxonomy name and its corresponding average abundance value.

receptor while *K. marxianus* JLU-1016 and AR strain JLU-1016A reversed all these parameters (Figure 10(h)). The related molecular mechanisms remain unclear. These results suggest that *K. marxianus* may be a potential probiotic in the prevention of the development of KI.

Apoptosis is the pathogenetic mechanism of KI, and attenuating apoptosis is an effective approach to prevent KI development [42]. *K. marxianus* also attenuated the apoptotic situation of the KI model in the present study. However, the exact mechanism has yet not been well understood. *K. marxianus* has seldom been reported to have the effects on the apoptosis, but it can affect the richness of *Lactobacillus*, which may be a potential strain to control the apoptosis development in kidney diseases [43]. Creatinine is an important biomarker during the pathogenesis of kidney disease and also affected by *K. marxianus* treatment, which may also be caused by the regulation of *Lactobacillus* [44]. KI implies danger signaling and a response by the release of mature IL-1β, which is a central element of inflammation and in turn promotes KI progression [45]. IL-6 signaling plays an important role in acute and CHD [46, 47]. *K. marxianus* treatment reduced the inflammatory

cytokine levels of IL-1β and IL-6, which is consistent with the report that *K. marxianus* has anti-inflammatory potential [44], and its treatment may be beneficial to improve gut inflammation since gut is a source of inflammation in CHD [48]. The inflammatory TLR4/NF-κB axis promotes KI development and progression [14, 49], and the inhibition of the signaling pathways has been widely reported to control KI development [15, 50]. The present findings also approved that *K. marxianus* treatment shows protective function for KI by downregulating the expression of TLR4/NF-κB (Figure 9). Gut microbiota mediates TLR4/NF-κB signaling pathway [51], and *Lactobacillus* also affects the pathway [52]. *K. marxianus* possibly affects the expression of TLR4/NF-κB via the modulation of gut microbiota. To prove that, much work still needs to be done in the future.

There were some limitations to the present study. OGTT test was not performed strictly for a small size ($n = 3$ for each group) although the plasma glucose levels reached the peak at 15 min after the oral load of glucose, and differences were insignificant among the four groups at the most time, suggesting that the results were stable with little random errors. Anti-inflammatory properties were not measured in our study, although a similar scenario was conceivable from the poor induction of kidney IL-1β, IL-6, and TNF-α. All these important issues should be solved in the future work.

4.1. Future Studies. K. marxianus JLU-1016 and JLU-1016A dietary supplement are protected against metabolism-related KI and apoptosis. Apoptosis is a complicated process by regulating the destruction of kidney cells. Pro and antiapoptotic markers such as Bax (a proapoptotic factor) [53], Bcl-2 (an antiapoptotic factor) [54], cytochrome c (an antiapoptotic factor) [55], caspase-3 (a proapoptotic factor) [56], and mothers against decapentaplegic homolog 3 (SMAD3) (a cellular apoptosis inducer) [57] were involved with the complex processes of KI. However, the antiapoptotic activities of the strains were justly roughly evaluated via a TUNEL analysis (Figure 4). All these marker genes and protein expression studies should be performed in the KI model. Furthermore, AR strain JLU-1016A showed the higher improvement in KI severity, apoptosis, lipid profile, and creatinine levels when compared with the non-acid-resistant strain JLU-1016. AR strain JLU-1016A may be more efficacious than the non-acid-resistant strain supplements because of gastric-acid resistant and better survival. Strong acid-resistant strains were found in the fecal flora of healthy adults when compared with the patients with ulcerative colitis (UC), suggesting that such acid-resistant strains may reduce inflammatory symptoms [58]. The other acid-resistant probiotics showed higher efficiency in lipid and carbohydrate metabolism [59]. All the relevant experiments have not been tested by using the present acid-resistant strain in the KI model yet. The exact molecular mechanisms should be explored in the future work.

5. Conclusions

K. marxianus JLU-1016 and AR strain JLU-1016A diets protected against metabolism-related KI, apoptosis, glucose tolerance, inflammation, and downregulation of the inflammation-related TLR4/NF-κB signaling pathway. HFD induction increased the proportion of *Firmicutes* but reduced the proportion of probiotics *Bacteroidetes* and *Lactobacillus*. *K. marxianus* JLU-1016 and JLU-1016A strain treatments reduced the proportion of *Firmicutes* and increased the proportion of *Bacteroidetes* and *Lactobacillus* in the KI model. *K. marxianus* diet might have a beneficial effect on KI by improving anti-inflammatory, antiapoptosis, and glucose tolerance properties and increasing the proportion of probiotics.

Data Availability

All data supporting this work are included within the paper.

Conflicts of Interest

The authors declare that there is no conflict of interest.

Authors' Contributions

NL and GZ performed the experiments, interpreted the data, and wrote the manuscript. MX designed the study, performed the data analysis, and revised the manuscript. NL and GZ contributed to the study design and revising and editing the manuscript.

References

[1] T. Liu, X. Liang, C. Lei et al., "High-fat diet affects heavy metal accumulation and toxicity to mice liver and kidney probably via gut microbiota," *Frontiers in Microbiology*, vol. 11, p. 1604, 2020.

[2] S. Ha, Y. Yang, B. M. Kim et al., "Activation of PAR2 promotes high-fat diet-induced renal injury by inducing oxidative stress and inflammation," *Biochimica et Biophysica Acta (BBA) - Molecular Basis of Disease*, vol. 1868, no. 10, article 166474, 2022.

[3] T. Kobayashi, Y. Iwata, Y. Nakade, and T. Wada, "Significance of the gut microbiota in acute kidney injury," *Toxins*, vol. 13, no. 6, p. 369, 2021.

[4] J. Gong, S. Noel, J. L. Pluznick, A. R. A. Hamad, and H. Rabb, *Gut microbiota-kidney cross-talk in acute kidney injury*, Elsevier, 2019.

[5] S. Maccaferri, A. Klinder, P. Brigidi, P. Cavina, and A. Costabile, "Potential probiotic Kluyveromyces marxianus B0399 modulates the immune response in Caco-2 cells and peripheral blood mononuclear cells and impacts the human gut microbiota in an in vitro colonic model system," *Applied and Environmental Microbiology*, vol. 78, no. 4, pp. 956–964, 2012.

[6] V. Navarro-López, A. Hernández-Belmonte, M. I. Soto et al., "Oral intake of Kluyveromyces marxianus B0399 plus lactobacillus rhamnosus CECT 30579 to mitigate symptoms in COVID-19 patients: a randomized open label clinical trial," *Medicine in Microecology.*, vol. 14, article 100061, 2022.

[7] A. Lisotti, R. Enrico, and G. Mazzella, "Su2037 effects of a fermented milk containing Kluyveromyces marxianus B0399 and Bifidobacterium lactis BB12 in patients with irritable bowel

syndrome: a new effective agent," *Gastroenterology*, vol. 144, no. 5, pp. S-538–S-539, 2013.

[8] D. E. Romanin, S. Llopis, S. Genovés et al., "Probiotic yeastKluyveromyces marxianusCIDCA 8154 shows anti-inflammatory and anti-oxidative stress properties inin vivomodels," *Beneficial Microbes*, vol. 7, no. 1, pp. 83–93, 2016.

[9] S. Mirdamadi, M. Mirzaei, N. Soleymanzadeh, M. Safavi, N. Bakhtiari, and M. Zandi, "Antioxidant and cytoprotective effects of synthetic peptides identified from *Kluyveromyces marxianus* protein hydrolysate: insight into the molecular mechanism," *LWT*, vol. 148, article 111792, 2021.

[10] É. Galinari, J. Almeida-Lima, G. R. Macedo, H. C. Mantovani, and H. A. O. Rocha, "Antioxidant, antiproliferative, and immunostimulatory effects of cell wall α-d-mannan fractions from *Kluyveromyces marxianus*," *International Journal of Biological Macromolecules*, vol. 109, pp. 837–846, 2018.

[11] S. Wang, X. Song, K. Zhang et al., "Overexpression of toll-like receptor 4 affects autophagy, oxidative stress, and inflammatory responses in monocytes of transgenic sheep," *Frontiers in Cell and Development Biology*, vol. 8, p. 248, 2020.

[12] K.-i. Sugiyama, M. Muroi, M. Kinoshita et al., "NF-κB activation via MyD88-dependent toll-like receptor signaling is inhibited by trichothecene mycotoxin deoxynivalenol," *The Journal of Toxicological Sciences*, vol. 41, no. 2, pp. 273–279, 2016.

[13] X. Peng, Y. Wang, H. Li et al., "ATG5-mediated autophagy suppresses NF-κB signaling to limit epithelial inflammatory response to kidney injury," *Cell Death & Disease*, vol. 10, no. 4, pp. 1–16, 2019.

[14] Y. Zhong, S. Wu, Y. Yang et al., "LIGHT aggravates sepsis-associated acute kidney injury via TLR4-MyD88-NF-κB pathway," *Journal of Cellular and Molecular Medicine*, vol. 24, no. 20, pp. 11936–11948, 2020.

[15] S. Guo, L. Guo, Q. Fang et al., "Astaxanthin protects against early acute kidney injury in severely burned rats by inactivating the TLR4/MyD88/NF-κB axis and upregulating heme oxygenase-1," *Scientific Reports*, vol. 11, no. 1, pp. 1–16, 2021.

[16] A. Oeckinghaus and S. Ghosh, "The NF-kappaB family of transcription factors and its regulation," *Cold Spring Harbor Perspectives in Biology*, vol. 1, no. 4, article a000034, 2009.

[17] S. Kim, S. A. Lee, H. Yoon et al., "Exosome-based delivery of super-repressor IκBα ameliorates kidney ischemia- reperfusion injury," *Kidney International*, vol. 100, no. 3, pp. 570–584, 2021.

[18] B. Corcoran, C. Stanton, G. Fitzgerald, and R. Ross, "Survival of probiotic lactobacilli in acidic environments is enhanced in the presence of metabolizable sugars," *Applied and Environmental Microbiology*, vol. 71, no. 6, pp. 3060–3067, 2005.

[19] C. Du, Y. Li, X. Zhao et al., "The production of ethanol from lignocellulosic biomass by Kluyveromyces marxianus CICC 1727-5 and Spathaspora passalidarum ATCC MYA-4345," *Applied Microbiology and Biotechnology*, vol. 103, no. 6, pp. 2845–2855, 2019.

[20] R. Benedé-Ubieto, O. Estévez-Vázquez, P. Ramadori, F. J. Cubero, and Y. A. Nevzorova, "Guidelines and considerations for metabolic tolerance tests in mice," *Diabetes, Metabolic Syndrome and Obesity*, vol. Volume 13, pp. 439–450, 2020.

[21] J. He, X. Shen, D. Fu et al., "Human periodontitis-associated salivary microbiome affects the immune response of diabetic mice," *Journal of Oral Microbiology*, vol. 14, no. 1, p. 2107814, 2022.

[22] C. Xu, X. Huang, G. Yan, D. Wang, M. Hu, and C. Tang, "Tolvaptan improves contrast-induced acute kidney injury," *Journal of the Renin-Angiotensin-Aldosterone System*, vol. 2022, article 7435292, pp. 1–9, 2022.

[23] L. Wang, Y. Tan, Z. Zhu et al., "ATP2B1-AS1 promotes cerebral ischemia/reperfusion injury through regulating the miR-330-5p/TLR4-MyD88-NF-κB signaling pathway," *Frontiers in Cell and Development Biology*, vol. 9, p. 9, 2021.

[24] Y. Yu, M. Li, B. Xu et al., "A study of regulatory effects of TLR4 and NF-κB on primary biliary cholangitis," *European Review for Medical and Pharmacological Sciences*, vol. 23, no. 9, pp. 3951–3959, 2019.

[25] F. F.-Y. Lee, K. Davidson, C. Harris, J. McClendon, W. J. Janssen, and S. Alper, "NF-κB mediates lipopolysaccharide-induced alternative pre-mRNA splicing of *MyD88* in mouse macrophages," *Journal of Biological Chemistry*, vol. 295, no. 18, pp. 6236–6248, 2020.

[26] H. Esmaili Gourvarchin Galeh, S. Meysam Abtahi Froushani, N. Afzale Ahangaran, and S. N. Hadai, "Effects of educated monocytes with xenogeneic mesenchymal stem cell–derived conditioned medium in a mouse model of chronic asthma," *Immunological Investigations*, vol. 47, no. 5, pp. 504–520, 2018.

[27] L. Lahti and S. Shetty, *Introduction to the Microbiome R Package*, 2018, https://bioconductor.statistik.tu-dortmund.de/packages/3.6/bioc/vignettes/microbiome/inst/doc/vignette.html.

[28] A. Ravi, P. Troncoso-Rey, J. Ahn-Jarvis et al., "Hybrid metagenome assemblies link carbohydrate structure with function in the human gut microbiome," *Communications biology.*, vol. 5, no. 1, pp. 1–13, 2022.

[29] J. A. Oksanen, F. G. Blanchet, M. Friendly et al., "Vegan: community ecology package," *R Package Version*, vol. 2, no. 5–7, p. 2022, 2020.

[30] R. Kindt and M. R. Kindt, "Package biodiversity R," *Package For Community Ecology And Suitability Analysis*, vol. 2, pp. 11-12, 2019.

[31] C.-H. Gao, G. Yu, and P. Cai, "ggVennDiagram: an intuitive, easy-to-use, and highly customizable R package to generate venn diagram," *Frontiers in Genetics*, vol. 12, 2021.

[32] T. Ma, R. Zaheer, T. A. McAllister et al., "Expressions of resistome is linked to the key functions and stability of active rumen microbiome," *Animal Microbiome*, vol. 4, no. 1, pp. 1–17, 2022.

[33] Z. Gu and M. Z. Gu, "Global options I," *Package 'Circlize'*, 2022.

[34] P. J. McMurdie and S. Holmes, *Package 'Phyloseq'*, Tech. Rep. Stanford Univ, Stanford, CA, USA, 2019.

[35] R. Matos, I. Amorim, A. Magalhães, F. Haesebrouck, F. Gärtner, and C. A. Reis, "Adhesion of Helicobacter species to the human gastric mucosa: a deep look into glycans role," *Frontiers in Molecular Biosciences*, vol. 8, article 656439, 2021.

[36] A. Bahadori, C. De Witte, M. Agin et al., "Presence of gastric helicobacter species in children suffering from gastric disorders in southern Turkey," *Helicobacter*, vol. 23, no. 5, article e12511, 2018.

[37] R. Matos, H. S. Sousa, J. Nogueiro et al., "Helicobacter species binding to the human gastric mucosa," *Helicobacter*, vol. 27, no. 1, article e12867, 2022.

[38] I. J. P. Garcia, J. S. Cézar, B. S. Lemos et al., "Effects of high fat diet on kidney lipid content and the Na, K-ATPase activity,"

Brazilian Journal of Pharmaceutical Sciences, vol. 54, no. 1, p. 54, 2018.

[39] J. Liu, Z. He, N. Ma, and Z.-Y. Chen, "Beneficial effects of dietary polyphenols on high-fat diet-induced obesity linking with modulation of gut microbiota," *Journal of Agricultural and Food Chemistry*, vol. 68, no. 1, p. 33, 2020.

[40] A. Zaky, S. J. Glastras, M. Y. Wong, C. A. Pollock, and S. Saad, "The role of the gut microbiome in diabetes and obesity-related kidney disease," *International Journal of Molecular Sciences*, vol. 22, no. 17, p. 9641, 2021.

[41] S. H. Suh, T. R. Oh, H. S. Choi et al., "Association of body weight variability with adverse cardiovascular outcomes in patients with pre-dialysis chronic kidney disease," *Nutrients*, vol. 13, no. 10, p. 3381, 2021.

[42] Q. Lin, S. Li, N. Jiang et al., "Inhibiting NLRP3 inflammasome attenuates apoptosis in contrast-induced acute kidney injury through the upregulation of HIF1A and BNIP3-mediated mitophagy," *Autophagy*, vol. 17, no. 10, pp. 2975–2990, 2021.

[43] Y.-S. Tsai, Y.-P. Chen, S.-W. Lin, Y.-L. Chen, C.-C. Chen, and G.-J. Huang, "*Lactobacillus rhamnosus* GKLC1 ameliorates cisplatin-induced chronic nephrotoxicity by inhibiting cell inflammation and apoptosis," *Biomedicine & Pharmacotherapy*, vol. 147, article 112701, 2022.

[44] S. M. Ghoreishy, N. Shirzad, M. Nakhjavani, A. Esteghamati, K. Djafarian, and A. Esmaillzadeh, "Effect of daily consumption of probiotic yoghurt on albumin to creatinine ratio, eGFR and metabolic parameters in patients with type 2 diabetes with microalbuminuria: study protocol for a randomised controlled clinical trial," *BMJ Open*, vol. 12, no. 3, article e056110, 2022.

[45] Y. Lei, S. K. Devarapu, M. Motrapu et al., "Interleukin-1β inhibition for chronic kidney disease in obese mice with type 2 diabetes," *Frontiers in Immunology*, vol. 10, p. 1223, 2019.

[46] H. Su, C.-T. Lei, and C. Zhang, "Interleukin-6 signaling pathway and its role in kidney disease: an update," *Frontiers in Immunology*, vol. 8, p. 405, 2017.

[47] A. L. Magno, L. Y. Herat, R. Carnagarin, M. P. Schlaich, and V. B. Matthews, "Current knowledge of IL-6 cytokine family members in acute and chronic kidney disease," *Biomedicine*, vol. 7, no. 1, p. 19, 2019.

[48] W. L. Lau, K. Kalantar-Zadeh, and N. D. Vaziri, "The gut as a source of inflammation in chronic kidney disease," *Nephron*, vol. 130, no. 2, pp. 92–98, 2015.

[49] X. Wang, J. Zhou, J. Yang, S. Wang, and L. Yang, "Role of TLR4/MyD88/NF-κB signaling in the contrast-induced injury of renal tubular epithelial cells," *Experimental and Therapeutic Medicine*, vol. 20, no. 5, pp. 1–1, 2020.

[50] P. Liu, F. Li, X. Xu et al., "1,25$(OH)_2D_3$ provides protection against diabetic kidney disease by downregulating the TLR4-MyD88-NF-κB pathway," *Experimental and Molecular Pathology*, vol. 114, article 104434, 2020.

[51] S. Shao, R. Jia, L. Zhao et al., "Xiao-Chai-Hu-Tang ameliorates tumor growth in cancer comorbid depressive symptoms via modulating gut microbiota-mediated TLR4/MyD88/NF-κB signaling pathway," *Phytomedicine*, vol. 88, article 153606, 2021.

[52] Y. Xia, Y. Chen, G. Wang et al., "*Lactobacillus plantarum* AR113 alleviates DSS-induced colitis by regulating the TLR4/MyD88/NF- κB pathway and gut microbiota composition," *Journal of Functional Foods*, vol. 67, article 103854, 2020.

[53] W. B. Yap, K. C. Goh, S. S. Hassan, and V. R. Balasubramaniam, "Regulation of pro-apoptotic Bax and trail gene expressions by H5N1 in Madin-Darby canine kidney (Mdck) cell line," *Pakistan Veterinary Journal*, vol. 40, no. 4, 2020.

[54] J. Nesovic Ostojic, M. Ivanov, N. Mihailovic-Stanojevic et al., "Hyperbaric oxygen preconditioning upregulates heme oxygenase-1 and anti-apoptotic Bcl-2 protein expression in spontaneously hypertensive rats with induced postischemic acute kidney injury," *International Journal of Molecular Sciences*, vol. 22, no. 3, p. 1382, 2021.

[55] L. Nežić, R. Škrbić, L. Amidžić et al., "Protective effects of simvastatin on endotoxin-induced acute kidney injury through activation of tubular epithelial cells' survival and hindering cytochrome C-mediated apoptosis," *International Journal of Molecular Sciences*, vol. 21, no. 19, p. 7236, 2020.

[56] J. Weng, Y. Wang, Y. Zhang, and D. Ye, "An activatable near-infrared fluorescence probe for in vivo imaging of acute kidney injury by targeting phosphatidylserine and caspase-3," *Journal of the American Chemical Society*, vol. 143, no. 43, pp. 18294–18304, 2021.

[57] X. Ji, H. Wang, Z. Wu et al., "Specific inhibitor of Smad 3 (SIS3) attenuates fibrosis, apoptosis, and inflammation in unilateral ureteral obstruction kidneys by inhibition of transforming growth factor β (TGF-β)/Smad 3 signaling," *Medical Science Monitor*, vol. 24, pp. 1633–1641, 2018.

[58] W. Wang, W. Xing, S. Wei et al., "Semi-rational screening of probiotics from the fecal flora of healthy adults against dss-induced colitis mice by enhancing anti-inflammatory activity and modulating the gut microbiota," *Journal of Microbiology and Biotechnology*, vol. 29, no. 9, pp. 1478–1487, 2019.

[59] G. Karimi, M. Saadat, S. Gheflat, B. Kazemi, and M. Bandehpour, "The effect of three acid-resistant isolated proteins from Lactobacillus casei on lipid and carbohydrate metabolism pathway-related genes: an in vitro study," *Biomedical and Biotechnology Research Journal*, vol. 5, no. 3, p. 276, 2021.